Journal of Chemical Engineering Research Studies

Research Article Open Access

Removal of Reactive Yellow 86 usingTiO_2 nanoparticle–colemanite waste

Eren T[1], Törün H[2], Yola ML[2], Ertan B[1] and Atar N[1*]

[1]Department of Chemistry, Dumlupinar University, Turkey

[2]Department of Metallurgical and Materials Engineering, Sinop University, Turkey

Abstract

A novel composite containingTiO_2 nanoparticles (TiO_2NPs) and colemanite waste (CW) was synthesized and tested in adsorption and photocatalysis to remove Reactive Yellow 86 (RY86) from aqueous solution. Transmission electron microscopy (TEM), X-ray photoelectron spectroscopy (XPS), and X-ray diffraction patterns (XRD) showed the formation of metal TiO_2 NPs on CW. The BET surface area increased after intercalation of TiO_2 NPs onto CW. TiO_2-CW was found to be a good nanomaterial for RY86 adsorption. The effects of operating variables such as initial dye concentration, pH and contact time in adsorption were studied. The kinetics, isotherm and thermodynamic parameters for the removal of the RY86 were also investigated. In addition, TiO_2-CW also shows high photocatalytic activity for degradation of RY86 from aqueous solution. The combination of adsorption and photocatalysis using TiO_2-CW is demonstrated as a more effective technique for removal of dyes from aqueous solution.

Keywords: Adsorption, photocatalysis ; TiO_2 nanoparticles, colemanite waste, kinetics.

Abbreviations : TiO_2 NPs-TiO_2 nanoparticles; CW- Colemanite waste; RY86-Reactive Yellow 86; TEM-Transmission electron microscopy; XPS-X-ray photoelectron spectroscopy; XRD-X-ray diffraction patterns; DRS- Diffuse reflectance spectrum; d-Density; λ-Wavelength, nm; t-Time, min; k1-Pseudo-first order rate constant, min-1; qe-Adsorption equilibrium capacity, mgg-1; qt - Amount of dye adsorbed, mgg-1; KF-Freundlich constant;Ce--Equilibrium dye concentration in solution, mgL-1; ΔG-Free energy change, kJ/mol; ΔS-Entropy change, J/molK; ΔH -enthalpy change, kJ/mol, T-Temperature, K; Kc-Adsorption equilibrium constant; Co-Initial dye concentration, mol/L; Ct- Dye concentration at t time, mol/L.

*Corresponding author: Atar N, Department of Chemistry, Arts and Science Faculty, Dumlupinar University, 43100, Kutahya, Turkey, Tel : +90-274-265-2051; Fax : +90-274-265-2056; E-mail: necipatar@gmail.com

Received May 04, 2014; Accepted June 24, 2014;Published September 1, 2014

Citation: Eren T, Törün H, Yola ML, Ertan B, Atar N (2014) Removal of Reactive Yellow 86 usingTiO2 nanoparticle-colemanite waste. Journal of Chemical Engineering Research Studies 1(1): 2.

Introduction

The pollution of water has been a serious problem in last decades [1] due to the presence of organic and inorganic pollutants from various industries such as plastics, textile, food and cosmetics. Removal of textile dyes from wastewater sources is important in water purification process. Recently, several techniques such as adsorption [2], biosorption [3], photocatalysis [4], chemical oxidation [5], anaerobic treatment [6] and membrane filtration [7] have been performed for the removal of textile dyes from wastewater. Adsorption has several advantages such as convenience, high removal efficiency and is straightforward to use of textile dyes containing wastewater [8]. Researchers have investigated various low-cost adsorbents such as clays [9], colemanite waste [10], fly ash [11], agricultural waste [12], bottom ash [13], bagasse pith [14], hen feathers [15], blast furnaces lag [16], fertilizer waste [17], red mud [18] and silkworm pupa [19]. In addition to adsorption technique, photocatalysis has also been an encouraging wastewater treatment technology. Because of the self-regenerated and reusable properties, photocatalysts such as WO_3, TiO_2, ZnS etc. has major advantages and a wide range of use than other treatment materials [20]. Among these photocatalysts, TiO_2 has been one of the most investigated photocatalysts over the last few decades, due to its high photocatalytic activity, redox properties, thermal and photochemical stability, commercially availability and non-toxicity in nature [21-24]. TiO_2 is also a conventional photocatalyst for the effective degradation of dyes [25, 26]. During the process, electrons can be stimulated from a photocatalyst for adsorbed dye decomposition. An ideal photocatalyst should be highly photoactive, stable and non-toxic and meet primary criteria for a higher H_2O/OH couple ($OH^- \rightarrow OH + e^-$, $E^0 = -2.8$ V) [27].

The boron ores are important natural resources in Turkey. During boron enrichment process, a large amount of colemanite ore waste (CW) is discharged into waste dams from the boron plants. The waste dams containing boron minerals can cause a big environmental problem. Colemanite ore waste contains colemanite, ulexite, zeolite, calcite and some clays. Colemanite is a boron mineral most found in Turkey with a basic formula "$CaB_3O_4(OH)_3 \bullet H_2O$" and it contains lots of $BO_2(OH)$ and $BO_3(OH)$. Previously, it has been demonstrated in many applications as a boron waste [8].

In this study, synthesis of TiO_2NPs with CW was performed without a reducing agent and their photocatalytic performance and adsorptive behaviour were investigated in the removal of RY86 in dye solutions with or without UV– vis irradiation. The results in our study have showed that the combination of adsorption and photocatalysis on TiO_2-CW is quite efficient technique for dye such as RY86 removal.

Materials and methods

Apparatus and reagents

CW was obtained from Etibor (Emet- Kütahya, Turkey). The chemical compositions of CW and TiO_2-CW were determined by inductively coupled plasma spectrophotometer (Perkin-Elmer Optima 4300 DW ICPOES). The absorption spectra of dye solutions were determined by a Shimadzu UV/Visible spectrophotometer (UV2550, Japan). TEM images were obtained on a JEOL 2100 HRTEM instrument (JEOL Ltd., Tokyo, Japan). XPS measurements were performed on a PHI 5000 Versa Probe (U ULVAC-PHI, Inc., Japan/USA) model spectrometer with a pressure of 10^{-7} Pa. X-ray diffraction (XRD) measurement of TiO_2-CW was performed with a Rikagu Miniflex X-ray diffractometer using mono-chromatic Cu Kα radiation. The BET surface areas of CW and TiO_2-CW were measured by N_2 adsorption–desorption (Quantachrome Corporation, NOVA-2000, USA). A diffuse reflectance spectrum (DRS) of TiO_2-CW was monitored on a UV-2550 Shimadzu UV– vis spectrophotometer equipped with ISR-2200 DRS accessory.

All chemicals were reagent grade and included the following: titanium isopropoxide ($Ti(OCH(CH_3)_2)_4$), (purity = 97%, d = 0.96 g mL^{-1}, Sigma-Aldrich), RY86 (Sigma-Aldrich). The aqueous solutions were prepared using ultra-pure quality of water with a resistance of 18.3 MΩ cm.

Preparation of TiO_2-CWphotocatalyst

The CW was firstly dried at 90 ºC for 48 h. After the CW dried, about 5 g of CW was added to 500 mL of ultra-pure water. This mixture was stirred for 1 h. 50 ml of 0.1 M $Ti(OCH(CH_3)_2)_4$ solution was prepared with ultra-pure water. The $Ti(OCH(CH_3)_2)_4$ solution was added to CW solution and kept with powerful stirring for 2 h. The mixture solution was centrifuged, washed with ultra-pure water, and dried in vacuum. Dried sample was calcined at 400 ºC for 4 h, under nitrogen flow. The TiO_2content of TiO_2-CW was nearly 14.1wt%.

Batch studies for adsorption

Stock RY86 dye solution at concentration of 1000 mg L^{-1} was prepared and it was diluted to obtain the experimental solutions. Batch experiments were performed in 50 mL flasks at 25 ºC in an isothermal shaker with a mixing speed of 200 rpm. The pH experiments were studied by shaking for 60 min at 25ºC, with 50 mg of TiO_2-CW in 50 mL of dye solution at different pH values. The solution pH was adjusted between 3.0-9.0 using 0.1 M HCl or NaOH and measured by a pH meter (Metler Toledo MA 235). Isothermal and kinetic studies were performed at 25ºC. In each run, 50 mg of TiO_2-CW was in contact with 50 mL of dye solution (25-200 mg L^{-1}) at different time intervals (10-110 min) at pH 3.0. The concentration of dye solution was analysed using a UV-Vis spectrophotometer at certain time intervals. The wavelength value for maximum absorbance (λ_{max}) of RY86 was observed at 416 nm, respectively. The concentrations of dye solution were calculated using the linear regression equations.

Photocatalytic oxidation of dyes

Photocatalytic degradation of RY86 was performed in a thermo static batch with a UV- vis lamp (400 W, λ = 250-570 nm) and quartz glass. The nitrogen gas was passed during degradation of the RY86. The photodegradation experiments were carried out in the above similar processes of adsorption.

Reusability experiments of TiO_2-CW for the adsorptive and photocatalytic removal of the reactive dyes

A serious of experiments was carried out to investigate the reusability of TiO_2-CWon the adsorptive and photocatalytic removal of the RY86. TiO_2-CW was reused five times and totally five experiments were performed with or without UV irradiation under similar conditions. Before next cycle of experiment, the catalyst was centrifuged at 12000 rpm for 8 min to separate it from the treated ultra-pure water. It is then washed five times with ethanol. Then, TiO_2-CW was dried at 100 ºC for 2h. Then next cycle of batch and photocatalytic degradation experiments was done and similar experimental conditions were used for all the five cycles.

Results and Discussion

Characterization of TiO_2-CW

The morphology of TiO_2-CWphotocatalyst was characterized using transmission electron microscopy with an accelerating voltage of 200 keV. The TEM image of TiO_2-CW is shown in Figure 1. Spherical shapedTiO_2NPs in the darker nucleus are uniformly extended on CW. The diameters of the spherical shaped TiO_2NPswere observed to be around 5-25 nm.

Figure 2 shows the XRD patterns of TiO_2-CW containing colemanite, zeolite, calcite phases of CW and anatase and rutile phases of TiO_2NPs. The peak at 21.07º is corresponded to zeolite, the peak at 30.08º is corresponded to calcite and the peaks at 24.62º, 27.53º, 35.81º and 48.16ºare corresponded to colemanite phases of CW, respectively. Also, the peak at 32.06º is corresponded to the rutile and the peaks at 25.31º, 38.12º, 47.36ºand 55.13º are corresponded to the anatase phases of TiO_2NPs, respectively [28].

In Figure 3, XPS characterization was performed to verify the formation of TiO_2 particles on CW. The XPS narrow region spectra and XPS survey have shown in Fig. 3. Peak signals for B_{1s}, Ca_{2p}, Ti_{2p}, and O_{1s}were observed in the survey spectrum of the CW have given as inset in Figure 3. O_{1s} peaks detected at around 510 eV were corresponded to O^{2-} of OH groups of boron minerals in CW. The Ti_{2p} peaks for TiO_2-CW were detected with a doublet $2p^{3/2}$ and $2p^{1/2}$ signals at 462.5 eV and 467.6 eV respectively [29]. These results indicate to the presence of TiO_2 in TiO_2-CW. The XPS spectra suggest the formation of TiO_2-CW by the reduction of Ti^{4+} ions using CW.

Figure 4 shows the DRS spectrum of TiO_2-CWthatobtained from subtracting the DRS spectrum of CW from the DRS spectrum of TiO_2-CW by using OriginPro8 software. The TiO_2-CW shows maximum visible light absorption at 570 nm. The visible light absorption of TiO_2-CW is due to the surface plasmon resonance of TiO_2NPs and it is strongly influenced by the metal oxides in CW.

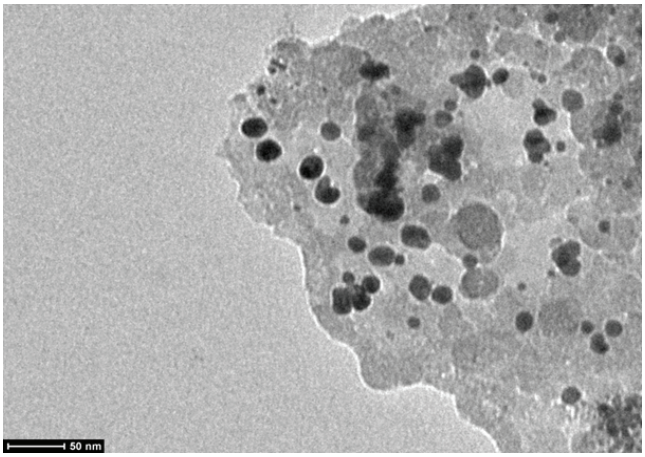

Figure 1. TEM image of TiO_2NPs formed on CW

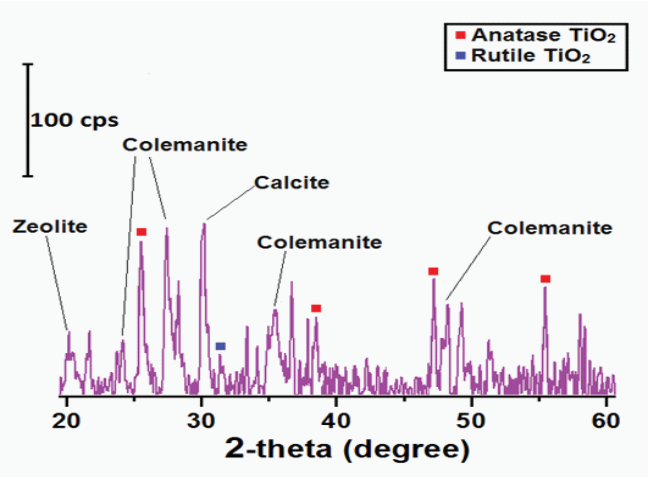

Figure 2. XRD spectra of synthesized TiO_2-CW

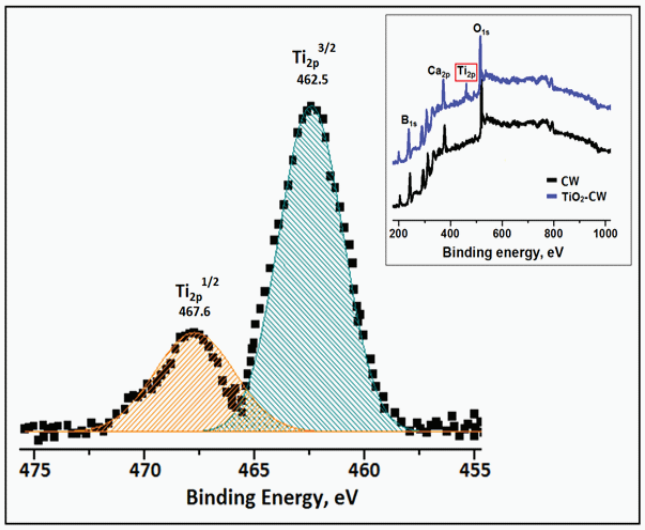

Figure 3. The narrow region XPS spectra of the TiO_2-CW (Inset is the XPS survey of the CW and TiO_2-CW)

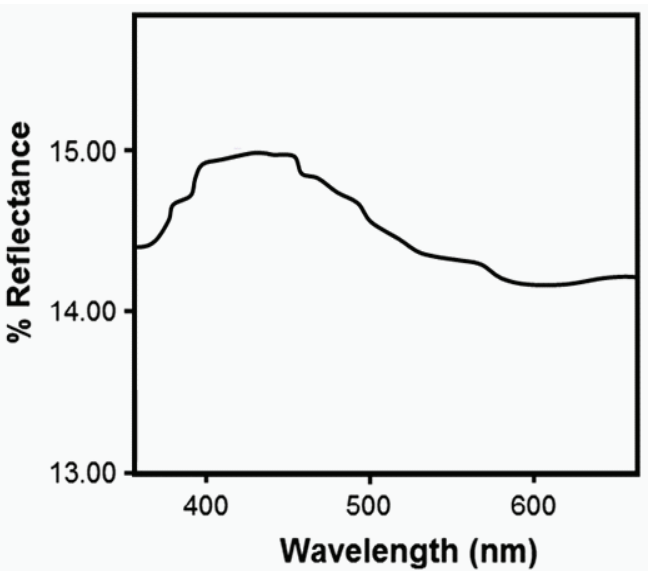

Figure 4. DRS spectrum of TiO_2-CW

Table 1 presents the chemical composition of TiO_2-CW. The chemical composition of the TiO_2-CW is including boron oxide, magnesium oxide, sulfate, calcium oxide, iron oxide, aluminium oxide and silicon dioxide as seen in Table 1.

Batch studies of dye adsorption

The effect of pH on the removal of RY86 from aqueous solution was examined without UV irradiation. Figure 5 shows the removal of RY86 using TiO_2-CWfrom aqueous solution. The uptake of RY86was reduced remarkably with increasing pH from 3.0 to 9.0 for adsorption. The maximum removal efficiency of the RY86 was observed at pH 3.0. The surface charge of TiO_2-CW has become more positive when the solution pH was decreased.

The effect of adsorbent dosage on the RY86uptakefrom aqueous solution was investigated in the range of 0.4– 2.0 g L^{-1}, at the initial RY86 concentration (150 mg L^{-1}), pH = 3 and contact time of 100 min. The uptake of RY86 using TiO_2-CWwas observed not to be increased after TiO_2-CW dosage of 1.0 g L^{-1}thus TiO_2-CWdosage of 1.0 g $L^{-1}$was chosen for all experiments (Figure not shown).

A series of experiments were performed at various time with a stable adsorbent amount of 1.0 g L^{-1}, pH of 3.0 and initial RY86 concentration of 150 mg L^{-1} to investigate the effect of contact time on the removal of RY86 from aqueous solution using TiO_2-CW. When the contact time was increased, the uptake levels of the RY86 were increased up to 100 min (Figure not shown). The initial adsorption rate for the RY86 was very rapid, because a large number of active sites are available for the adsorption. Two kinetic models were applied to the experimental data in this study. The Lagergren pseudo-first order model is shown by the equation [30];

$$\log(q_e - q_t) = \log q_e - (k_1 / 2.303)t \quad (1)$$

where $k_1$is the pseudo-first order rate constant (min^{-1}), q_e is the adsorption equilibrium capacity (mgg^{-1}), q_t is the amount of dye adsorbed (mgg^{-1}) at various time (t).

The equation stands for the integral form of the pseudo-second order model [31];

$$\frac{t}{q_t} = \frac{1}{k_2 q_2^2} + \frac{1}{q_2}t \quad (2)$$

where q_2 is the maximum adsorption capacity (mgg^{-1}); q_t is the amount of dye adsorbed per unit mass of the adsorbent (mgg^{-1}); k_2 is the rate constant of the pseudo-second order equation ($gmg^{-1}min^{-1}$). The equation means the non-linear form of equation (2);

$$q_t = \frac{q_2^2 k_2 t}{1 + q_2 k_2 t} \quad (3)$$

Table 2 shows the kinetic parameters. The correlation coefficient of the pseudo-first order model is lower than that of the pseudo-second order kinetic model for two systems. The results showed that the adsorption data of RY86 on TiO_2-CW were well fitted by the pseudo-second-order kinetic model. The pseudo-second order kinetic model is based on the rate limiting step which is chemical sorption or chemisorption involving valency forces [32].

Isotherm studies for the adsorption were carried out at various initial RY86 concentrations (10-200 mg L^{-1}) with a constant adsorbent dosage of 1.0 g L^{-1}, pH of 3.0 and contact time of 100 min. The Langmuir and Freundlich models are generally used to represent the adsorption process[33, 34].

The Langmuir isotherm means the monolayer coverage and the uniform energies of adsorption. The Langmuir equation is as follows

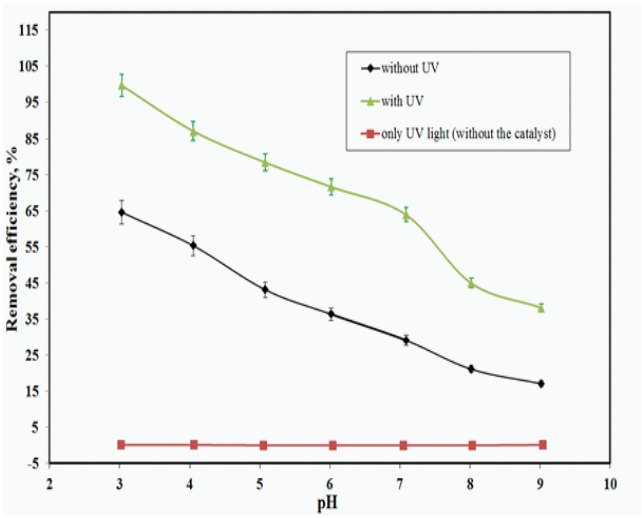

Figure 5. Effect of pH on the removal of RY86 from aqueous solution using TiO_2-CW

Table 1. Chemical composition of CW

Component	Chemical analysis (wt%)
CaO	17.64
SO_3	3.21
Fe_2O_3	1.87
Al_2O_3	3.12
B_2O_3	11.24
Na_2O	5.19
SiO_2	19.72
K_2O	2.08
MgO	8.31
Loss on ignition	27.62

Table 2. Kinetic parameters of the removal of the RY86 from aqueous solution

Dye solution	Pseudo-first order kinetic model			Pseudo-second order kinetic model		
	q_e (mg g^{-1})	k_1(min^{-1})	r_2^2	q_e(mg g^{-1})	k_2(g mg^{-1} min^{-1})	r_2^2
RY86 (with UV)	55.16	18.91	0.987	71.05	3.85×10^{-2}	0.998
RY86 (without UV)	44.39	14.06	0.953	59.88	1.67×10^{-2}	0.997

Table 3. Isotherm parameters of the removal of the RY86 from aqueous solution

Dye solution	Langmuir isotherm			Freundlich isotherm		
	q_{max} (mg g^{-1})	K_L (L mg^{-1})	r_L^2	K_F (mg g^{-1})	1/n	r_F^2
RY86 (with UV)	69.54	2.41×10^{-2}	0.996	53.05	0.39	0.894
RY86 (without UV)	51.06	1.51×10^{-2}	0.997	39.18	0.74	0.951

Table 4. Thermodynamic parameters

	ΔG^o (kj/mol)				ΔH^o (kj/mol)	ΔS^o (J/mol K)	r^2
	293 K	303 K	313 K	323 K			
RY86	-5.63	-5.42	-4.75	-3.82	-20.75	-68.09	0.992

[35]:

$$q_e = \frac{q_{\max} K_L C_e}{1 + K_L C_e} \quad (4)$$

$$\frac{1}{q_e} = \frac{1}{q_{\max}} + \left(\frac{1}{q_{\max} K_L}\right)\frac{1}{C_e} \quad (5)$$

where q_e is the equilibrium dye concentration (mgg^{-1}); $q_{\max}$, the monolayer capacity of the adsorbent (mgg^{-1}); K_L, the Langmuir constant and C_e, the equilibrium dye concentration in solution (mg L^{-1}).

The Freundlich isotherm is as follows [36]:

$$q_e = K_F C_e^{1/n} \quad (6)$$

$$\ln q_e = \ln K_F + \frac{1}{n} \ln C_e \quad (7)$$

where q_e is the equilibrium dye concentration on the adsorbent (mgg^{-1}); K_F, the Freundlich constant; C_e, the equilibrium dye concentration in solution (mgL^{-1}).In this model, the sorbent has a surface with a heterogeneous distribution of sorption heat.

Table 3 shows the adsorption isotherm parameters. The adsorption isotherms were L-curve in both systems (Figure not shown). The L-type curve shows the higher affinity of the adsorbate for the adsorbent [37]. The equilibrium data were well fitted to the Langmuir isotherm model (Table 3).

Thermodynamic parameters show applicability of adsorption process. Free energy change (ΔG), entropy change (ΔS) and enthalpy change (ΔH) were investigated. The adsorption equilibrium constant (K_c) is obtained by the equation;

$$K_c = \frac{C_d}{C_q} \quad (8)$$

C_d is the amount of dye (mg L^{-1}) adsorbed on the adsorbent and C_q is the equilibrium concentration (mgL^{-1}) of the dye in the solution. ΔG is given as follow;

$$\Delta G = -RT \ln K_c \quad (9)$$

The relationship between K_c and temperature (T) is shown by the Van`t Hoff equation;

$$\ln K_c = \frac{\Delta S}{R} - \left(\frac{\Delta H}{R}\right)\frac{1}{T} \quad (10)$$

Adsorption enthalpy (ΔH) and entropy (ΔS) values were obtained by the linear plot, ln Kc versus 1/T (Figure not shown). Table 4 shows the adsorption parameters of RY86 from aqueous solution. The negative values of ΔG are corresponded to spontaneous adsorption. The negative value of ΔH indicates the adsorption process is an exothermic process. The negative value of ΔS is corresponded to the decreased randomness at the solid–liquid interface during the adsorption.

Photocatalytic degradation of dyes

Photocatalytic degradation experiments of the RY86 were performed under UV light. In order to examine whether the degradation of RY86 was caused by photocatalysis, a series of experiments were also carried out without the catalyst in the presence of UV– vis radiation. The dye solution showed to be stable under UV–vis light and no degradation was observed without a photocatalyst as seen in Figure 5. Under UV– vis irradiation with TiO_2-CW, the higher RY86 degradation was observed and the removal efficiencies of the dye increased when the solution pH decreased (Figure 5), similar to that in adsorption. Compared with removal efficiencies in adsorption, photocatalytic removal efficiencies of RY86 are higher, suggesting the photocatalytic effectiveness of TiO_2-CW. The active sites of hydroxyl radicals of TiO_2-CW increase at lower pH values. Therefore, the catalyst has higher photocatalytic activity at lower pH values. The removal efficiencies (%) of RY86 were performed at various times (Figure not shown). The removal efficiency (%) of RY86 increased up to 100 min and reached to 99.70%. The reaction kinetic of the photocatalytic degradation of RY86 on TiO_2-CWwas evaluated using the first order kinetic model as follows [38]:

$$\ln C_t = \ln C_0 - kt \quad (11)$$

where C_o and C_t are initial dye concentration and dye concentration at t time, respectively. The first order rate constant (k) for the

photocatalytic degradation of RY86 was found to be 0.239 min^{-1}. Scheme 1 shows the photochemical mechanism. The band-gap value of TiO_2-CW was calculated using Tauc's approach [39] and it was found to be 3.08 eV.

The photocatalytic removal efficiencies (%) of RY86 are higher than the adsorptive removal efficiencies (%). The photocatalytic degradation efficiencies of RY86 occurred up to 99.70% within 100 min in the presence of UV– vis irradiation. But, the adsorptive removal efficiencies (%) of the RY86 occurred up to 64.51% within 100 min for adsorption without light. The reuse performance of TiO_2-CW for the adsorptive and photocatalytic removal of the RY86 from aqueous solutions was performed (Figure not shown). TiO_2-CW can be recycled and reused five times without much decline in removal efficiency. The good reusability of TiO_2-CW in the cyclic removal experiments shows that the adsorptive and photocatalytic property of TiO_2-CW is stable and practically important.

A comparison of the maximum photocatalytic activity of TiO2-CW with other catalysts is shown in Table 5. The results show that TiO2-CW presented higher dye removal efficiency than TiO2-based photocatalysts. The TiO2-CW material can be used as the alternative photocatalyst or adsorbent for the removal of reactive dyes from wastewater.

Conclusions

A novel photocatalyst containing TiO_2NPs and CW was synthesized and investigated in adsorption and photocatalysis to remove RY86 from aqueous solution. The photocatalyst was characterized by TEM, XRD and XPS. The removal of RY86 from aqueous solution using TiO_2-CW was found to be significantly dependent on solution pH (3.0), initial dye concentration (150 mg L^{-1}), contact time (80 min) and adsorbent dosage (1.0 g L^{-1}). The pseudo second-order kinetic model and the Langmuir isotherm were obtained to fit the adsorption experimental data. Thermodynamic parameters indicated exothermic and spontaneous reactions of the adsorption. The photocatalytic studies indicated TiO_2-CW shows high photocatalytic activity for degradation of the RY86from aqueous solution. The adsorption and photocatalysis experiments showed that TiO_2-CW can be efficiently, good reusability and economically used as an adsorbent or photocatalyst for the removal of the RY86 from aqueous solution.

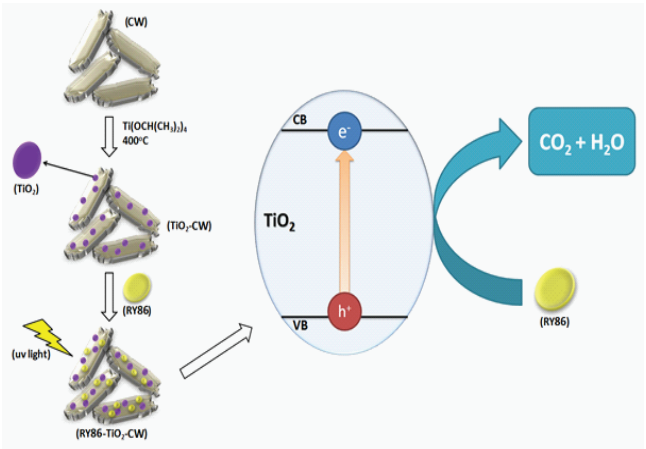

Scheme 1. Photochemical mechanism for the photodegradation of the reactive dyes using TiO_2-CW

Table 5. Comparison of photocatalytic degradation of dyes using various photocatalysts

Photocatlyst	Dye	Degradation (%)	Reference
Ti–SBA-15	Methylene blue	80.0	[38]
SiC–TiO_2	Methylene blue	52.0	[34]
N-TiO_2	RhB	33.0	[40]
P25	RhB	67.0	[40]
NG	AV	80.0	[40]
TiO_2 thin films	RB19	87.0	[41]
TiO_2 thin films	RY17	93.0	[41]
5SCT1	TB	60.8	[42]
P25-TiO_2	Rh6G	84.4	[42]
$SrCrO_4$	Rh6G	15.9	[42]
TiO_2-CW	RY86	99.7	This study

Acknowledgement

The authors would like to thank Dumlupinar University and Sinop University for support.

Conflict of interest

The authors declare no conflict of interest.

Authors' contributions

All authors have contributed equally.

References

1. Divband B, Khatamian M, Kazemi-Eslamian GR, Darbandi M. Synthesis of Ag/ZnO nanostructures by different methods and investigation of their photocatalytic efficiency for 4-nitrophenol degradation. Applied Surface Science. 2013; 284: 80–86.
2. Bhattacharyya KG, Sarma A. Adsorption characteristics of the dye, Brilliant Green, on Neem leaf powder. Dyes and Pigments. 2003; 57: 211–222.
3. Han R, Zou W, Yu W, Cheng S, Wang Y, Shi J. Biosorption of methylene blue from aqueous solution by fallen phoenix tree's leaves. J. Hazard.Mater. 2007; 141: 156–162.
4. Yuan R, Ramjaun SN, Wang Z, Liu J. Photocatalytic degradation and chlorination of azo dye in saline wastewater: kinetics and AOX formation. Chem. Eng. J. 2012; 192: 171–178.
5. Liang SH, Chen KF, Wu CS, Lin YH, Kao CM. Development of KMnO4-releasing composites for in situ chemical oxidation of TCE-contaminated groundwater. Water Res. 2014; 54: 149-158.
6. Alibardi L, Cossu R, Saleem M, Spagni A. Development and permeability of a dynamic membrane for anaerobic wastewater treatment. Bioresource Techn. 2014; 161: 236-244.
7. Barredo- Damas S, Alcaina-Miranda MI, Iborra- Clar MI, Mendoza-Roca JA. Application of tubular ceramic ultrafiltration membranes for the treatment of integrated textile wastewaters. Chem. Eng. J. 2012; 192: 211–218.
8. Atar N, Olgun A, Wang S. Adsorption of cadmium (II) and zinc (II) on boron enrichment process waste in aqueous solutions: Batch and fixed-bed system studies. Chem. Eng. J. 2012; 192: 1–7.
9. Auta M, Hameed BH. Modified mesoporous clay adsorbent for adsorption isotherm and kinetics of methylene blue, Chem. Eng. J. 2012; 198–199: 219– 227.
10. Yola ML, Eren T, Atar N, Wang S. Adsorptive and photocatalytic removal of reactive dyes by silver nanoparticle-colemanite ore waste. Chem. Eng. J. 2014; 242: 333–340.
11. Rameshraja D, Srivastava VC, Kushwaha JP, Mall ID. Quinoline adsorption onto granular activated carbon and bagasse fly ash. Chem. Eng. J. 2012; 181–182: 343–351.

12. Djilani C, Zaghdoudi R, Modarressi A, Rogalski M, Djazi F, Lallam A. Elimination of organic micropollutants by adsorption on activated carbon prepared from agricultural waste. Chem. Eng. J. 2012; 189–190: 203–212.

13. Gupta VK, Mittal A, Krishnan L,Gajbe V. Adsorption kinetics and column operations for the removal and recovery of malachite green from wastewater using bottom ash. Sep. Sci. Technol. 2004; 40: 87–96.

14. Allen SJ, Murray M,Brown P, Flynn O. Peat as an adsorbent for dyestuffs and metals in wastewater. Resour. Conserv.Recycl. 1994; 11: 25–39.

15. Mittal A, Malviya A, Kaur D,Mittal J, Kurup L. Studies on the adsorption kinetics and isotherms for the removal and recovery of Methyl Orange from wastewaters using waste materials. J. Hazard. Mater. 2007; 148: 229–240.

16. Ramakrishna KR, Viraraghavan T. Use of slag for dye removal. Waste Manage. 1997; 17: 483–488.

17. Jain AK, Gupta VK, Bhatnagar A, Suhas. Utilization of industrial waste products as adsorbents for the removal of dyes. J. Hazard. Mater.2003; 101: 31–42.

18. Zhang L, Liu N,Yang L, Lin Q. Sorption behavior of nano-TiO_2 for the removal of selenium ions from aqueous solution. J. Hazard. Mater.2009; 170: 1197–1203.

19. Noroozi B, Sorial GA, Bahrami H,Arami M. Equilibrium and kinetic adsorption study of a cationic dye by a natural adsorbent—silkworm pupa. J. Hazard. Mater.2007; 139: 167–174.

20. Beydoun D, Amal R, Low G, McEvoy S. Role of Nanoparticles in Photocatalysis. J. Nanopart. Res. 1999; 1: 439-458.

21. Pekakis PA, Xekoukoulotakis NP, Mantzavinos D. Treatment of textile dyehouse wastewater by TiO2 photocatalysis. Water Res. 2006; 40: 1276–1286.

22. Bessekhouad Y, Chaoui N, Trzpit M, Ghazzal N, Robert D, Weber JV.UV-vis versus visible degradation of acid orange II in a coupled CdS/TiO2 semiconductors suspension. J. Photochem. Photobiol. A: Chem. 2006; 183: 218–224.

23. Dostanić J, Grbić B, Radić N, Stefanov P, Šaponjić Z, Buha J, et al. Photodegradation of an azopyridone dye using TiO_2 films prepared by the spray pyrolysis method. Chem. Eng. J. 2012; 180: 57-65.

24. Pan L,Zou JJ, Wang S, Huang ZF, Zhang X, Wang L. Enhancement of visible-light-induced photodegradation over hierarchical porous TiO_2 by non-metal doping and water-mediated dye sensitization. Appl. Surf. Sci. 2013; 268: 252-258.

25. Gazi S, Rajakumar A, Pradeep Singh ND. Photodegradation of organic dyes in the presence of [Fe(III)-salen]Cl complex and H2O2 under visible light irradiation. J. Hazard. Mater. 2010; 183: 894–901.

26. Velmurugan R, Swaminathan M. An efficient nanostructured ZnO for dye sensitized degradation of Reactive Red 120 dye under solar light. Sol. Energy Mater.Sol. Cells. 2011; 95: 942–950.

27. Hoffmann MR, Martin ST, Choi W, Bahnemann DW. Environmental applications of semiconductor photocatalysis. Chem. Rev. 1995; 95: 69–96.

28. Mohamed- Mokhtar M., Asghar BHM, Muathen HA. Facile synthesis of mesoporous bicrystallized TiO2(B)/anatase (rutile) phases as active photocatalysts for nitrate reduction. Catalysis Communications.2012; 28: 58–63.

29. Velmurugan R, Krishnakumar B, Subash B, Swaminathan M. Preparation and characterization of carbon nanoparticles loaded TiO_2 and its catalytic activity driven by natural sunlight. Sol. Energy Mater.Sol. Cells. 2013; 108: 205–212.

30. Atar N, Olgun A. Removal of basic and acid dyes from aqueous solutions by a waste containing boron impurity. Desalination. 2009; 249: 109–115.

31. Ho YS, McKay G. Kinetic Models for the Sorption of Dye from Aqueous Solution by Wood. Process Saf. Environ. Prot. 1998; 76: 183-191.

32. Olgun A, Atar N. Equilibrium and kinetic adsorption study of Basic Yellow 28 and Basic Red 46 by a boron industry waste. J. Hazard. Mater. 2009; 161: 148–156.

33. Shen D, Fan J, Zhou W, Gao B, Yue Q, Kang Q. Adsorption kinetics and isotherm of anionic dyes onto organo-bentonite from single and multisolute systems. J. Hazard. Mater.2009; 172: 99-107.

34. Gómez-Solís C, Juárez-Ramírez I, Moctezuma E, Torres-Martínez LM. Photodegradation of indigo carmine and methylene blue dyes in aqueous solution by SiC–TiO2 catalysts prepared by sol–gel. J. Hazard. Mater.2012; 217–218: 194-199.

35. Langmuir I. The adsorption of gases on plane surfaces of glass, mica and platinum. J. Am. Chem. Soc. 1918; 40: 1361-1403.

36. Freundlich H. Uberdie adsorption in Losungen. Z. Phys. Chem. 1906; 57: 385-470

37. Atar N, Olgun A, Wang S, Liu S. Adsorption of anionic dyes on boron industry waste in single and binary solutions using batch and fixed-bed systems. J. Chem. Eng. Data. 2011; 56: 508–516.

38. Das SK, Bhunia MK, Bhaumik A. Highly ordered Ti-SBA-15: efficient H2 adsorbent and photocatalyst for eco-toxic dye degradation.J. Solid State Chem. 2010; 183: 1326–1333.

39. Tauc J, Grigorovici R, Vancu A. Optical properties and electronic structure of amorphous germanium. Phys. Status Solidi B. 1966; 15: 627–637.

40. CharanpahariA, Umare SS, Sasikala R.Visiblelight active N doped GeO2 for the photodegradation of both anionicandcationicdyes. Catal. Commun. 2013; 40: 9-12.

41. FagnernN, LeotphayakkaratR, Chawengkijwanich C, Gleeson MP, Koonsaeng N, Sanguanruang S. Effect of titanium-tetraisopropoxide concentration on the photocatalytic efficiency of nanocrystalline thin films TiO2 used for the photodegradation of textile dyes. J. Phys. Chem. Solids 2012; 73: 1483-1486.

42. GhoraiTK, BiswasN. Photodegradation of rhodamine 6G in aqueous solution via SrCrO4 and TiO2 nano-sphere mixed oxides. J. Mater. Res. Technol. 2013; 2: 10-17.